Research Article

Stabilising control strategy for cyber-physical power systems

Etinosa Ekomwenrenren[1], Hatem Alharbi[1], Taisir Elgorashi[1], Jaafar Elmirghani[1], Petros Aristidou[1] ✉

[1]Department of Electronic and Electrical Engineering, Institute of Communication and Power Networks, University of Leeds, Leeds, LS2 9JT, UK
✉ E-mail: p.aristidou@leeds.ac.uk

Abstract: The cyber-physical nature of electric power systems has increased immensely over the past decades, with advanced communication infrastructure paving the way. It is now possible to design wide-area controllers, relying on remote monitor and control of devices that can tackle power system stability problems more effectively than local controllers. However, their performance and security relies extensively on the communication infrastructure and can make power systems vulnerable to disturbances emerging on the cyber side of the system. In this study, the authors investigate the effect of communication delays on the performance of wide-area damping controllers designed to stabilise oscillatory modes in a cyber-physical power system (CPPS). They propose a rule-based control strategy that combines wide-area and traditional local stabilising controllers to increase the performance and maintain the stable operation of CPPS. The proposed strategy is validated on a reduced CPPS equivalent model of Great Britain.

Nomenclature

The parameters and variables used to model the IP over WDM network are:

Parameters:

s and d	indices of the source and destination nodes
m and n	indices of the end nodes of a physical link
N	set of nodes
Nm_m	set of neighbouring nodes of the node m
Dr	router processing delay
Dt	transponder processing delay
De	EDFA amplifying delay
Ds	optical switching delay
W	number of wavelengths per fibre
B	wavelength data rate
S	maximum span distance between two EDFAs
D_{mn}	distance of the physical link (m, n)
A_{mn}	number of EDFAs on the physical link (m, n) given as $$A_{mn} = \frac{D_{mn}}{S - 1}$$
L_{sd}	traffic demand from node s to node d
$\mathcal{C}$	speed of light

Variables:

F_{mn}	number of fibres in the physical link (m, n)
L_{mn}^{sd}	amount of traffic flow between node pair (s, d) traversing the physical link (m, n)
δ_{mn}^{sd}	$\delta_{mn}^{sd} = 1$, if demand (s, d) traverses a physical link (m, n); otherwise, $\delta_{mn}^{sd} = 0$
Ne_{sd}	number of EDFAs on the path traversed by demand (s, d)
h_{sd}	number of hops of the path traversed by demand (s, d)
$\mathcal{D}\text{prop}_{sd}$	total propagation delay of the path traversed by demand (s, d)
$\mathcal{D}\text{comp}_{sd}$	total components delay on the path traversed by demand (s, d)
d_{sd}	total delay experienced by demand (s, d)

1 Introduction

As electric power systems move toward a low-carbon energy future, the demand for higher sustainability leads to the decommissioning of conventional fossil-fuel generators and their replacement with intermittent and predominantly power-electronic-interfaced renewable energy sources. This transformation leads to power systems with lower inertia, where phenomena can propagate faster, and leaves the system with fewer resources to tackle stability problems since these were traditionally provided by conventional generation units. In addition, the introduction of new, disruptive technologies into power systems modifies their behaviour and might cause new stability problems. Finally, the need for increased efficiency drives power systems to operate closer to their stability limits, relying more and more on real-time operational strategies to ensure system security.

At the same time, electric power networks are quickly developing into cyber-physical power system (CPPS) [1], with communication infrastructure playing a dominant role [2, 3]. Advances in remote communication and sensing with the use of global positioning system (GPS) synchronised phasor measurement units have allowed for the development of new wide-area monitoring systems able to receive, process, and visualise information from large-scale power systems [4]. Owing to this improved situational awareness, real-time monitoring of the CPPS dynamic health is a possibility, thus reducing the likelihood of outages and catastrophic blackouts [5, 6].

Furthermore, this advanced communication infrastructure can provide improved remote control capabilities, providing an ideal platform for wide-area damping controllers (WADCs) designed to tackle oscillatory problems in the system and enhance its stability [6–9]. Such WADCs exploit the communication infrastructure of CPPS to provide better interconnection of grid components and assets dispersed across wide geographical areas [10].

WADCs can be designed to stabilise oscillatory modes in power systems, especially inter-area oscillations. Badly damped oscillations can limit the power transferred through tie lines, decreasing the security margins and increasing economic cost. To the extreme, lightly damped or unstable inter-area modes affect the system security and may result in catastrophic system-wide failures [7, 11]. WADCs with better observation capabilities can damp inter-area oscillations more effectively than traditional power system stabilisers (PSSs), which only use local information [7]. This is especially true for some cases where inter-area modes may be observable from one area but controllable from a different area [12].
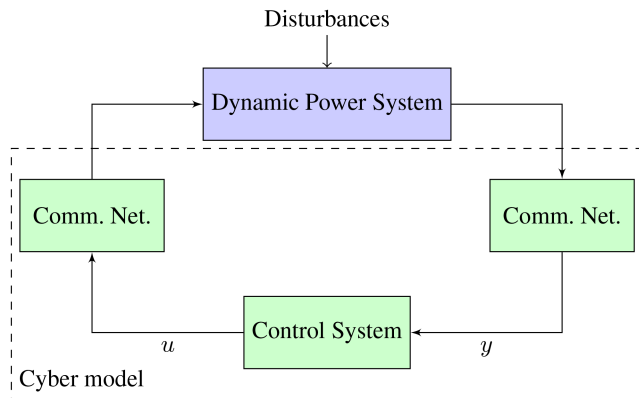
Fig. 1 *Abstract model of the CPPS*

However, WADCs (such as all geographically dispersed control systems) rely strongly on the communication infrastructure used to receive/send the monitoring and control signals. Dedicated communication infrastructure, used only for the needs of the power system monitoring and control, can have high reliability, low latency, and increased performance, with fewer security considerations. However, the cost of such an infrastructure is usually prohibitive. On the contrary, using the existing-commercial-communication infrastructure is more cost-effective but introduces high uncertainty concerning the performance of the communication system and increased cyber-security concerns. One of the major concerns is the communication latency caused by increased background communication or a cyber-attack. This may result in the degradation of the WADC performance, cause system instability [7] and adversely affect the overall security of the CPPS. Hence, it is important to analyse the stability of the resulting, time-delayed, CPPS, and protect against such events [13]. By providing robustness to the parametric uncertainty coming from communication time delays, the security of the CPPS can be significantly improved.

1.1 Related work

The stability of the CPPS in the presence of time delays is usually analysed using either time or frequency-domain methods. In the time-domain analysis, methods based on the Lyapunov functionals have been employed to derive the delay-dependent stability criteria of power systems [14–16]. However, Lyapunov-based methods only give sufficient conditions for stability [17] and can prove computationally challenging in large-scale systems. In the frequency domain, the eigenvalues of the system have been used to assess its stability after the time delays have been approximated as a rational polynomial [18–20]. Alternatively, spectral discretisation methods have also been employed [17, 21]. Gao *et al.* [22] showed that eigenanalysis methods based on approximating the time delays using Padé approximations are sufficiently accurate and more efficient than an explicit spectra discretisation scheme [21].

Several methods have been proposed in the literature for compensating time delays in wide-area control schemes. Chaudhuri *et al.* [13] and Zabaiou *et al.* [23] compensate for fixed time delays during the control design stage using the Smith predictor approach. In [24], a gain scheduling technique was proposed via linear matrix inequalities (LMIs) to design a parameter-dependent controller that compensates for time delays within a certain tolerance. Other works, e.g. [25–27], also compensate for fixed time delays by extending the models using Padé approximations. These works, however, do not investigate or design for situations when the time delays greatly exceed the tolerance range of the designed controllers.

In [13], continuous latency compensation is provided by accounting for the phase shift caused by the time delays using an adaptive controller, while in [28] lead–lag compensators are used. Although these works compensate for time-varying delays, the performance of the system could become compromised in emergency situations such as a failure of a communication link or cyber-attacks creating abnormally large time delays [29], which

may cause failure of the wide-area controllers and compromise power system stability. Finally, most of the works do not explicitly consider the underlying communication architecture in a combined, CPPS model.

1.2 Paper contributions

In this paper, we investigate stabilising control strategies for CPPSs with the use of WADC and under the effect of communication latency. The contribution of this paper is split into four areas.

First, a CPPS model of Great Britain (GB) is developed, suitable for the design and assessment of WADCs. A reduced dynamic model of GB transmission network (TN) is developed based on existing, validated, static model, and using standard engineering practises for the dynamic components. The power system model is then overlaid with the British Telecoms (BT) core fibre network [BT 21st century (BT 21CN)]. Then, an optimisation-based algorithm is developed to compute the communication latency between the nodes under different conditions.

Second, a WADC is designed to stabilise the CPPS using H_∞-based techniques with regional pole placement. The performance of the WADC is studied both with eigenvalue analysis and time-domain simulations. Then, the WADC sensitivity to communication latency, causing time delays in the measurement and control signals, is assessed.

Third, a hybrid controller is proposed using a combination of wide-area and local controls to improve the system's resiliency to communication latency. The WADC tackles the slower but harder to control locally inter-area modes, whereas the faster modes are tackled by PSS controllers.

Finally, a rule-based strategy is proposed to combine the superior performance of the WADC in situations of low latency, with the increased resilience of the hybrid approach in cases of high latency, and the robustness of traditional local controls in cases of communication failure.

The rest of this paper is organised as follows: in Section 2, the developed CPPS is presented along with the time-delayed system used in this work. The modelling and computations of the communication system are detailed in Section 3. In Section 4, the basic principles behind the techniques used for the design of the H_∞-based WADCs are presented. Section 5 describes the development of the WADC, the hybrid control, and the rule-based control strategy. Some simulation results are also shown in the same section. Finally, conclusions are drawn in Section 6.

2 CPPS modelling

In this section, we present the modelling aspects of the study model which consists of a dynamic power system model and an overlaying communication network.

In general, CPPSs are modelled as hybrid systems [30], that is, dynamical systems that exhibit both continuous and discrete dynamic behaviour. The continuous model represents the non-linear electric power system dynamic behaviour while the discrete model represents the digital control and communication systems. For this reason, CPPSs are challenging to model, simulate, and analyse. Many solutions have been proposed in the past for coupling the cyber and physical sides for simulation purposes [31].

In this work, the hybrid model of Fig. 1 is considered for the development of the WADC and the simulation of the CPPS. The power, control, and communication systems were co-simulated in MATLAB/Simulink. The communication system model, as detailed in Section 3, was developed in MATLAB. For simulation, this model was implemented as a sub-component in Simulink. The measured signals pass through the communication sub-component and the time-delayed measurement signal is received at the controller input. The controlled signal is transmitted similarly. For the sensitivity analysis, a Padé approximation of the time delays was used.

The dynamic power system model is described in Section 2.1, whereas the communication model in Section 3. The WADC design is described in Section 4.
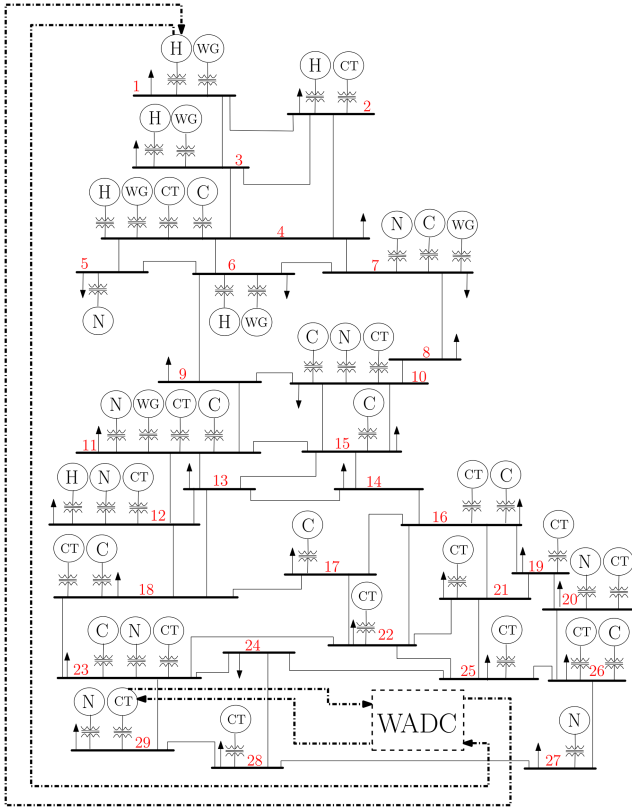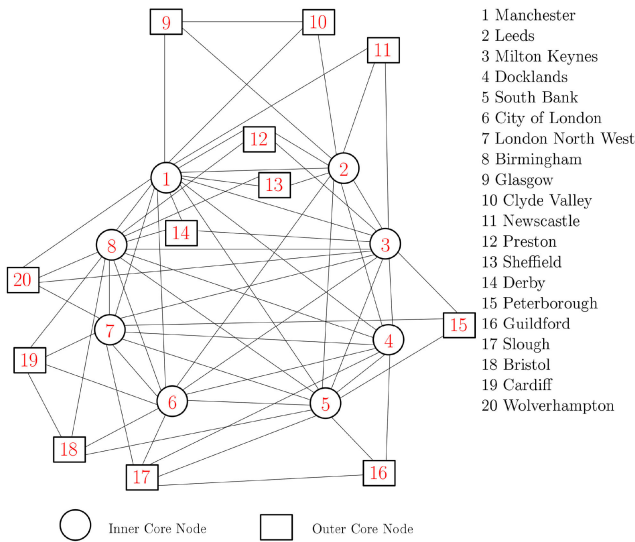
Fig. 2 *Representative GB TN with WADC*

1 Manchester
2 Leeds
3 Milton Keynes
4 Docklands
5 South Bank
6 City of London
7 London North West
8 Birmingham
9 Glasgow
10 Clyde Valley
11 Newscastle
12 Preston
13 Sheffield
14 Derby
15 Peterborough
16 Guildford
17 Slough
18 Bristol
19 Cardiff
20 Wolverhampton

○ Inner Core Node   □ Outer Core Node

Fig. 3 *BT (UK) fibre core network [35, 36]*

2.1 Representative GB TN system

Fig. 2 shows the reduced dynamic model of the GB high-voltage TN used in this work. It consists of 29 buses, 99 transmission lines (98 double and one single circuit), and 65 generators with a total installed capacity of ~75 GW. The generators consist of hydro (H), nuclear (N), coal (C), combine-cycle gas turbine (CT), and wind power plants wind generation (WG), and are located on 24 buses as shown in this figure. This model shows the main transmission routes and was based on the static (AC power flow) model of [32]. It maintains all the critical characteristics and the generation mixture and loading conditions were preserved.

For the dynamic model, all of the conventional power plants (H, N, C, CT) were modelled with sixth-order synchronous generators [33] while the WGs with Type-1 fourth-order squirrel cage induction generators. Moreover, the IEEE ST1A excitation system and the steam/hydro turbine models provided by MATLAB, and
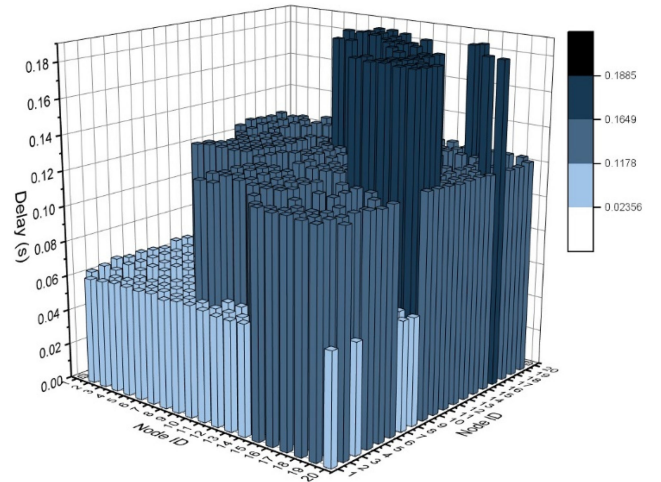

Fig. 4 *Communications delay between BT 21CN nodes*

originating from [34], were used for each synchronous generator. The default (suggested) parameters were used for these models.

2.2 BT (UK) fibre core network

The overlaying communication system for the CPPS is based on the BT 21CN fibre core network [35, 36], and sketched in Fig. 3. The fibre core network was utilised because of the stringent communication requirements in current power grid services [37]. Owing to the high reliability needed in the power grid, very demanding quality of service (QoS) is required of the communication architecture including in terms of latency. Moving to a commercially available fibre network would allow reducing the cost while guaranteeing the necessary QoS.

The BT 21CN core network contains 20 nodes interconnected by 68 links. The core nodes consist of 8 inner and 12 outer core nodes. The 8 inner core nodes are fully meshed while the 12 outer nodes are connected to a minimum of three other nodes. The upshot of this is that some nodes are not directly connected to each other. Since the communication delay (Section 3) is made up of both component delays (mostly due to routing) and signal propagation delay (due to physical distance and length of optical fibre), the total time delay between any two nodes not directly connected together is larger than the delays between nodes directly connected to each other. The communication delay between each pair of the BT 21CN nodes is shown in Fig. 4. The relative locations of the power system nodes in the representative GB model in relation to the BT 21CN core nodes were determined approximately and the assumption that each power node is connected directly to the closest core node was made.

Since the focus of this work is the effect of communication latency on the performance of WADCs, the behaviour of the CPPS can be captured as a time-delayed power system with a centralised controller, as sketched in Fig. 5. To compute the time delays appearing in the CPPS, an appropriate communication system model has been developed and is detailed in Section 3. The resulting time-delayed system can then be used in the WADC control design.

3 Communication system

Reducing time delay is an essential factor in communication networks to ensure the QoS.

The Internet protocol (IP) is the main communication protocol in the IP suite for exchanging packets in interconnected networks. The IP over wavelength division multiplexing (WDM) network [38] is the architecture of choice in core network because of the high data rate supported by WDM through carrying multiple wavelengths on a single fibre. The IP over WDM network consists of two layers: the IP layer and the optical layer (Fig. 6). In the IP layer, the IP router is used in each node to aggregate traffic from access networks connecting end users. The optical layer provides the large bandwidth required to support data communication
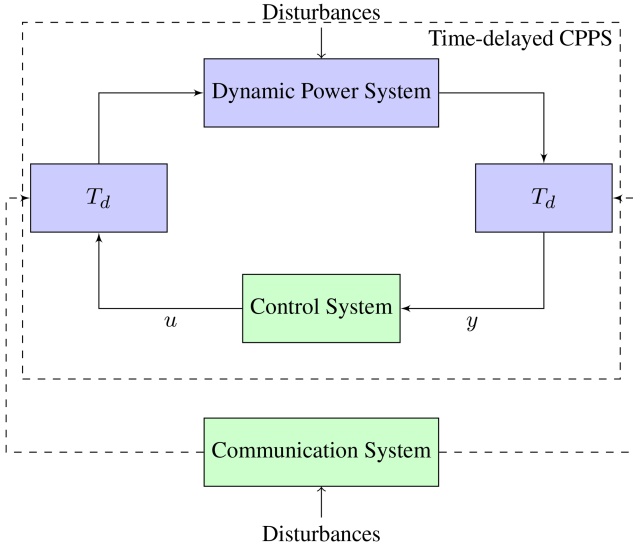
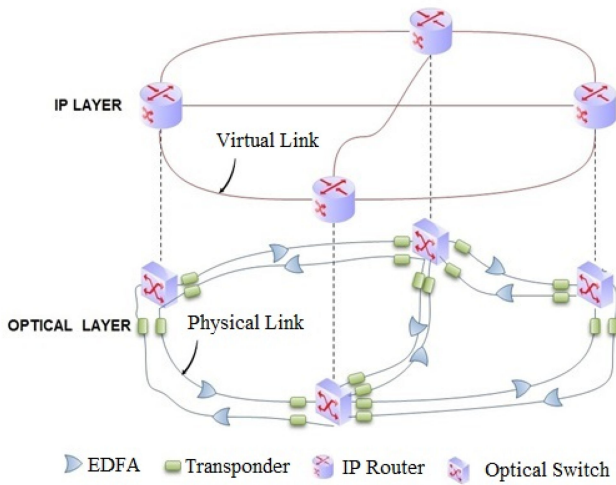**Fig. 5** *Time-delayed CPPS*

Fig. 6 *IP over WDM network architecture*

between IP routers. The IP router is connected to the optical layer through an optical switch. The optical switch is connected to the fibre links. The transponders provide optical-electronic-optical (OEO) conversion. The erbium-doped fibre amplifiers (EDFAs) are placed in fibre links to enable long-distance transmission of the optical signals. In addition to optical switching and OEO conversion, IP traffic is processed and forwarded by IP routers at all intermediate nodes of its path in the current implementation of IP over WDM networks.

In communication networks, traffic flows experience delays at different points [39]. The time required to place all the bits of a packet into the transmission link is referred to as transmission delay. Network components contribute to the delay. In the IP over WDM architecture, traffic will experience processing delay at routers and transponders, switching delay at optical switches and amplifying delay at EDFAs. Traffic packets also experience queuing delay in buffers waiting to be processed or transmitted. The travel time through the transmission medium is referred to as the propagation delay. In optical fibre links, the propagation delay is constrained by the speed of light. In our paper, we only consider components delay and propagation delay.

3.1 Mixed integer linear programming (MILP) model

In this section, we present an MILP model used to optimise the routing of traffic so the time delays appearing in the CPPS due to disturbances in the communication network are minimised.

3.1.1 Objective: The objective is to minimise the delay between node pairs

$$d_{sd} = \mathscr{D}\text{prop}_{sd} + \mathscr{D}\text{comp}_{sd}, \quad \forall s, d \in N \tag{1}$$

3.1.2 Flow conservation constraint: This represents the flow conservation constraint. It ensures that the total incoming traffic equals the total outgoing traffic in all nodes, excluding the source and destination nodes

$$\sum_{n \in Nm_m} L_{mn}^{sd} - \sum_{n \in Nm_m} L_{mn}^{sd} = \begin{cases} L_{sd} & m = s \\ -L_{sd} & m = d \\ 0 & \text{otherwise} \end{cases} \tag{2}$$

$$\forall s, d, m \in N : s \neq d$$

3.1.3 Capacity constraint: This ensures that the traffic flow in a link does not exceed the capacity of wavelengths in its fibres

$$\sum_{s \in N} \sum_{d \in N : s \neq d} L_{mn}^{sd} \leq \text{WBF}_{mn}, \quad \forall m, n \in N \tag{3}$$

3.1.4 Components delay constraint: Constraints (4)–(8) calculate the delay resulting from different IP over WDM components on the paths selected to route demands. Constraints (4) and (5) relate the variable (L_{mn}^{sd}) to the binary variable (δ_{mn}^{sd}). Constraints (6) and (7) calculate the number of EDFAs and the number of hops on the path of each demand. Constraint (8) calculates the total components delay of paths

$$L_{mn}^{sd} \geq \delta_{mn}^{sd}, \quad \forall s, d, m, n \in N : s \neq d \tag{4}$$

$$L_{mn}^{sd} \leq L\delta_{mn}^{sd}, \quad \forall s, d, m, n \in N : s \neq d \tag{5}$$

$$Ne_{sd} = \sum_{m \in N} \sum_{n \in N : m \neq n} \delta_{mn}^{sd} A_{mn}, \quad \forall s, d \in N \tag{6}$$

$$h_{sd} = \sum_{m \in N} \sum_{n \in N : m \neq n} \delta_{mn}^{sd}, \quad \forall s, d \in N \tag{7}$$

$$\mathscr{D}\text{comp}_{sd} = h_{sd}(Dr + DeNe_{sd} + Dt + Ps), \quad \forall s, d \in N \tag{8}$$

3.1.5 Propagation delay constraint: This calculates the total propagation delay of the path of each demand

$$\mathscr{D}\text{prop}_{sd} = \sum_{m \in N} \sum_{n \in N : m \neq n} \frac{\delta_{mn}^{sd} D_{mn}}{\mathscr{C}}, \quad \forall s, d \in N \tag{9}$$

3.1.6 MILP formulation: Under the non-bypass routing approach, the overall MILP is modelled as

$$\begin{aligned} &\min \quad (1) \\ &\text{subject to} \quad (2) - (9) \end{aligned}$$

3.2 BT (GB) core network model calculations

Table 1 shows the MILP model input parameters. The physical distance between two EDFAs is considered to be 80 km and a single fibre link carries 16 wavelengths each of 40 Gbps. The components delay is dominated by the optical switching delay.

Fig. 4 shows the delay between the BT 21CN core nodes. The optimum route that results in minimum delay is the minimum hop route. This is due to the dominance of the delay contributed by the network components. The delay is, therefore, determined by the number of hops, where each node contains optical switches, routers, and transponders. The propagation delay is smaller in comparison and is determined by the length of the routes (routes are amplified by EDFAs which do not add any significant latency), and links in the BT 21CN do not exceed 360 km. Therefore, all demands are routed based on the minimum hop. Therefore, we
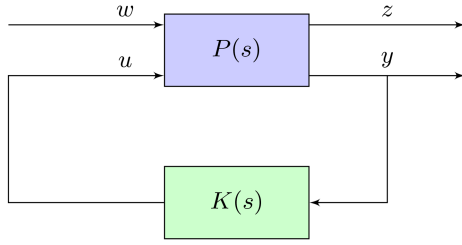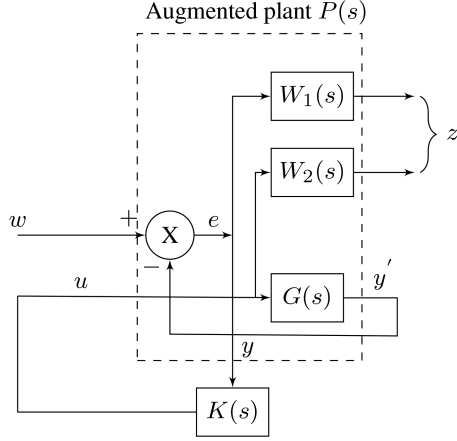
Fig. 7 *Generalised two-port plant diagram*

Fig. 8 *Illustration of mixed sensitivity*

have three levels of delay reflecting the three hop counts between node pairs in BT 21CN network (one hop, two hops and three hops).

4 H_∞ Control

This section briefly describes the principles of H_∞ control used in the design of the WADC.

Robust control techniques based on H_∞ methods have been previously used to design WADCs in the literatures [7, 13, 45]. For a linear system with a transfer function $E(s)$, its H_∞ norm is the highest gain of the transfer function over all frequencies and input directions [46]. It can thus be expressed as

$$\| E(s) \|_\infty \triangleq \max_\omega \overline{\sigma}(E(j\omega)) \tag{10}$$

where $\overline{\sigma}$ represents the maximum singular value.

In Fig. 7, $P(s)$ is the transfer function of the plant and $K(s)$ that of the controller. In this work, the plant is the power system to be stabilised and the controller refers to the WADC. Let $P(s)$ has the following realisation [47, 48]:

$$\dot{x} = Ax + B_1 w + B_2 u \tag{11}$$

$$z = C_1 x + D_{11} w + D_{12} u \tag{12}$$

$$y = C_2 x + D_{21} w + D_{22} u \tag{13}$$

where w is the disturbance vector; x is the state vector; y is the observation vector; z is the error vector; and the control vector is represented as u [48].

That is, the partitioned plant P can be represented as [47, 48]

$$P(s) = \begin{bmatrix} A & B_1 & B_2 \\ C_1 & D_{11} & D_{12} \\ C_2 & D_{21} & D_{22} \end{bmatrix} = \begin{bmatrix} P_{11}(s) & P_{12}(s) \\ P_{21}(s) & P_{22}(s) \end{bmatrix}$$

and the closed-loop transfer function from w to z is given as [47]

$$T_{wz}(s) = P_{11}(s) + P_{12}(s)K(s)(I - P_{22}(s))^{-1}P_{21}(s) \tag{14}$$

Table 1 BT 21CN model input parameters

number of wavelengths in a fibre (W)	16 [40]
bit rate of each wavelength (B)	40 Gbps [40]
span distance between two EDFAs (S)	80 km
speed of light ($\mathscr{C}$)	299,792 km/s
core router processing delay (Dr)	100 µs [41]
transponder processing delay (Dt)	10 µs [42]
EDFA amplifying delay (De)	50 µs [43]
optical switching delay (Ds)	60 ms [44]

The H_∞ problem involves designing a controller that internally stabilises the controlled system and makes

$$\| T_{wz}(s) \|_\infty < \gamma \tag{15}$$

for a given scalar γ [46–48].

4.1 Mixed-sensitivity H_∞ synthesis

In this work, the mixed-sensitivity H_∞ synthesis, depicted in Fig. 8, is used to design a stabilising controller $K(s)$. This method allows for shaping the sensitivity function $[S(s)]$ and the complementary sensitivity function $[K(s)S(s)]$ of the closed-loop system to achieve design targets compatible with good performance and robustness [46]. To achieve this, the controller must minimise

$$\left\| \begin{bmatrix} W_1(s)S(s) \\ W_2(s)K(s)S(s) \end{bmatrix} \right\|_\infty \tag{16}$$

where $G(s)$ is the open-loop transfer function of the system to be controlled, the sensitivity $S(s) = [I + G(s)K(s)]^{-1}$ is the transfer function from the disturbance vector w to the observation vector y and $K(s)S(s)$ measures the control effort [46].

For output disturbance rejection, a low-pass filter, $W_1(s)$, is usually used and $W_2(s)$ is a high-pass filter chosen to minimise the control effort at higher frequencies [46].

The mixed-sensitivity problem is converted into the standard H_∞ problem by computing an augmented plant, $P(s)$, formed from the open-loop transfer function and the weighting functions [46]. The solution to the H_∞ problem is to find all the controllers that stabilise the system internally and satisfy (15). In this work, the LMIs approach is used to solve the H_∞ problem using the robust control toolbox in MATLAB. Additional constraints are specified to place the poles of the controlled system in a specified region on complex s-plane. This region is specified by a conic sector lying in the left-hand plane having its tip at the origin and with its inner angle specified in terms of the minimum damping ratio [46].

5 Problem formulation and control design in the GB CPPS

In this section, the analysis and design of the controls for the CPPS of Section 2 is presented. It has to be noted that while the controls are introduced through the specific CPPS model, the methodology is general and can be easily adapted to other systems.

In Section 5.1, the analysis of the open-loop, uncontrolled system is shown to motivate the control design and serve as a benchmark. In Section 5.2, the design of the H_∞-based WADC is described, assuming no time delays and its resilience to communication latency is investigated. In Section 5.3, the design of a hybrid scheme (WADC and local PSS) is shown along with its increased robustness to communication time delays and different loading conditions. Finally, the rule-based switching control strategy is explained in Section 5.4.

5.1 Initial analysis

The system depicted in Fig. 4 can be generally modelled using delayed differential algebraic equations (DDAEs). To analyse the
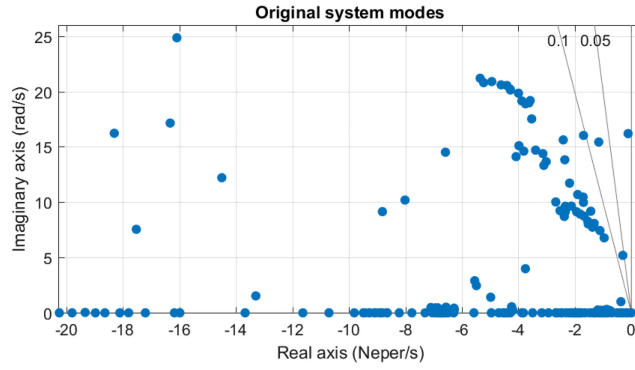
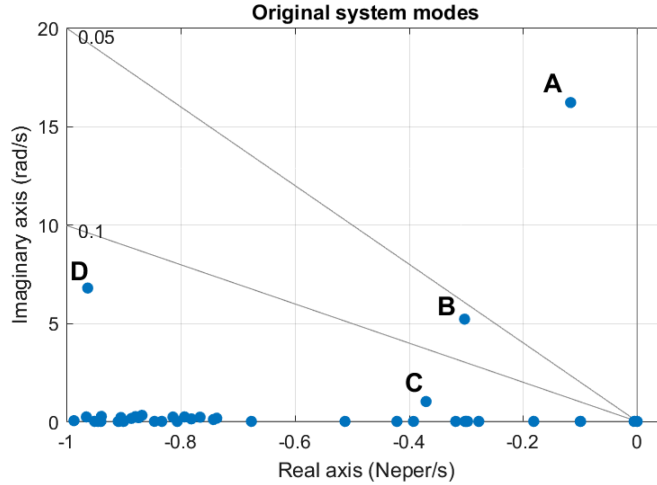**Fig. 9** *Eigenvalues of the uncontrolled power system model*

Fig. 10 *Critical system modes of the uncontrolled power system model*

Table 2 Critical system modes of uncontrolled power system model

Mode label	Eigenvalue	Frequency, Hz	Damping, %	Mode description
A	$-0.1165 \pm j16.1938$	2.58	0.72	intra-station
B	$-0.3024 \pm j5.1925$	0.83	5.81	inter-area
C	$-0.3699 \pm j1.0082$	0.16	34.44	global
D	$-0.9627 \pm j6.772$	1.08	14.07	inter-area

system performance and enable the design of the WADC, the DDAE model is linearised around the operating point and the delays (considered constant in this work) are treated using the Padé approximation [21].

A good damping ratio for power system damping evaluation is usually system dependent and based on practical rules but a damping ratio of 5% is typically acceptable [49]. Accordingly, a well-damped system should have a damping ratio of at least 5%, with all the eigenvalues corresponding to the system modes lying in the left half of the *s*-plane. The damping ratio from eigenvalue analysis will be used for evaluating the power system damping.

First, the open-loop (uncontrolled) power system model is linearised around the operating point, resulting in a linear model with 797 states. Fig. 9 shows the *s*-plane plot of the eigenvalues (modes) of the linearised system. The vertical distance of the modes indicates their frequency of oscillation and further to the left of the imaginary axis the modes are, the lesser the effect they have on the system's transient response. The plot also reveals the existence of a poorly damped mode lying outside the 5% damping ratio line. It must be noted that for the uncontrolled system, the time delays do not affect the system stability.

The eigenvalues with real parts are >-1 are shown in Fig. 10. From the participation factor analysis [50], it can be seen that the four modes are all electromechanical and their details are given in Table 2. Modes C and D are well-damped, with damping ratios

above 10%, while mode A is poorly damped with a ratio of just 0.72%.

5.2 WADC design

In this section, a WADC is designed, based on the principles detailed in Section 4, to improve the damping of modes A and B in the study system. For this design, the system time delays are ignored. The reason is that designing a controller to be robust to a wide range of time delays (usually the worst-case delays) makes it very conservative (and unnecessarily restrictive). In our case, by using the rule-based control strategy (see Section 5.4), we can optimise around several smaller deadbands (in our case, three deadbands but could be extended) and be less conservative within each deadband.

First, the generator location and the controller input and output signals were selected, taking into consideration the controllability and observability of the system [46, 51]. The generators with the highest participation in the critical modes were selected as suitable locations. Moreover, the magnitude of the residues [51] was used to select the signals with the highest observability and controllability for modes A and B. Consequently, the rotor speed deviation and automatic voltage regulator (AVR) reference of the hydro generator at node 1 (Beauly) and the combined-cycle gas turbine (CCGT) generator at node 29 South West Peninsula (SWP) were selected.

Then, we proceed to the design of the H_∞-based WADC using mixed-sensitivity synthesis. A low-pass filter, $W_1(s)$, was selected to improve output disturbance rejection while a high-pass filter, $W_2(s)$, was used to reduce the control effort outside the frequency range of interest. The selected filters are

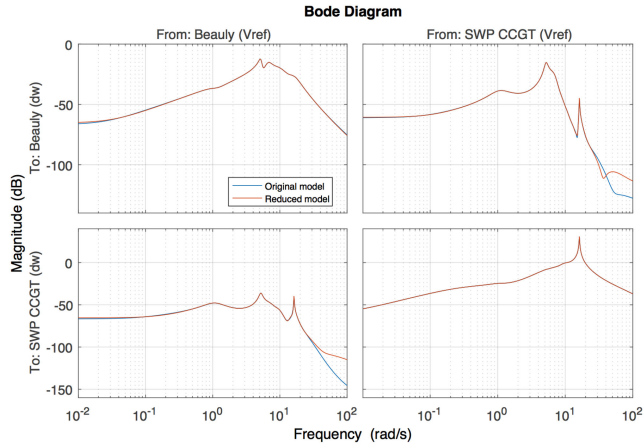$$W_1(s) = \frac{10}{s+10}, \quad W_2(s) = \frac{s}{s+100} \tag{17}$$

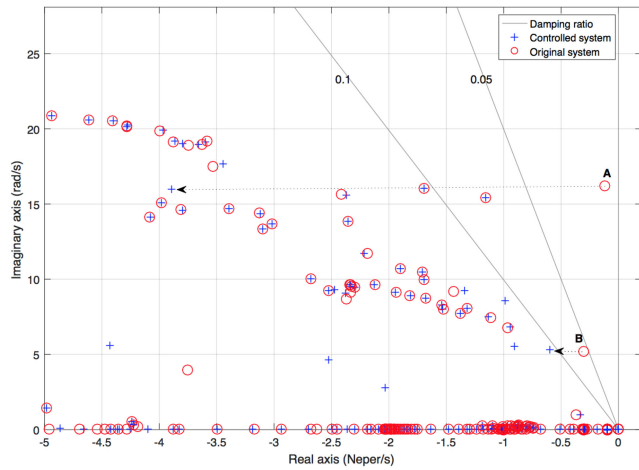**Fig. 11** *Frequency response of full and reduced order models*

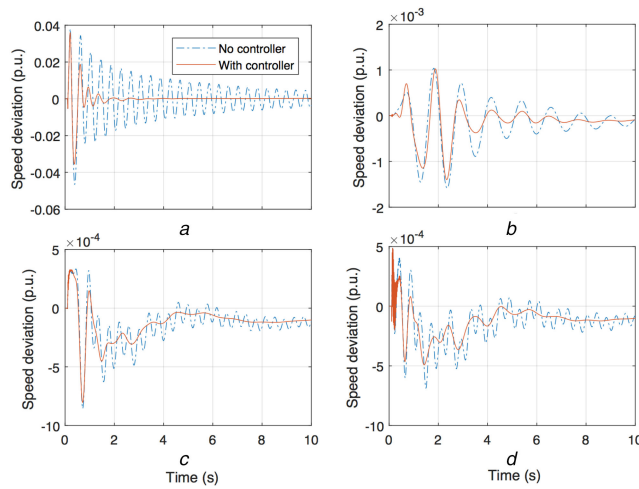**Fig. 12** *Comparison of eigenvalues between the uncontrolled and controlled (only WADC) system*

Fig. 13 *Generator speed of the uncontrolled and controlled (only WADC) system on*
(a) SWP (node 29) CCGT, *(b)* Beauly (node 1) hydro, *(c)* Keadby (node 16) coal, *(d)* Sellindge (node 27) nuclear

Before synthesising the controller, balance model reduction was used to decrease the model size to an equivalent model containing only 18 states. This was necessary to reduce the computational complexity and control effort [7, 46]. Fig. 11 shows the frequency response of both the reduced and full-order models for the frequency range of interest. As evidenced by the plot, the reduced model adequately approximates the full-order model within the frequency range of interest.

Finally, the H_∞-based WADC is synthesised using MATLAB Control Toolbox. The controller places the modes that are observable and controllable from the system output and input signals on the region of the complex s-plane that ensures a minimum damping ratio of 10%. This region on the complex s-plane is defined by a conic sector lying on the left of the s-plane with its tip at the origin and having an inner angle of $2 \times \cos^{-1}(0.1)$ rad.

From Fig. 12, it is observed that the damping of the system improves significantly with the WADC. The previously lightly damped mode A has been moved far into the left half plane, shortening the modes decay time. Also, the damping of inter-area mode B has been improved with a damping ratio of more than 10%. Modes C and D, however, remain relatively unchanged because of the choice of the controller input and output signals, which has limited observability and controllability of the modes. Nevertheless, this is acceptable as the modes were already adequately damped.

The small-signal response is verified via time-domain simulations of the full non-linear CPPS. A three-phase to ground short-circuit fault, cleared after one cycle (20 ms), was applied to the SWP node at $t = 0.1$ s to excite the oscillatory modes. The generator speed deviation is shown in Fig. 13. It can be seen that the system damping was poor before the introduction of the WADC, with the oscillation not completely decaying after 10 s. The system damping is significantly improved with the introduction of the WADC.

However, the performance of the WADC is sensitive to communication time delays. This is shown by performing a time-delay sensitivity analysis on the system. Constant time delays (T_d) are applied to the input and output paths of the controller communication links (Fig. 4) varying from 1 to 250 ms. For each step increase in time delay, the system is linearised around its initial operating point and its eigenvalues are extracted. An s-plane plot of the system eigenvalues for each of the time delays is shown in Fig. 14, where the green-through-red colour spectrum represents the increase in T_d from 1 to 250 ms.

The increase in time delays results in the eigenvalues moving toward the right hand of the complex s-plane, thereby worsening the mode damping ratio and increasing their decay time. For higher values of the time delays, the system reaches unstable operation as some eigenvalues eventually reach the right plane. Using the methodology explained in Section 2.2, we find that even for moderate background communication data, the time delays introduced might push the controlled system to instability.

To improve the resilience of the controlled CPPS to time delays, a hybrid control scheme combining a modified WADC operating together with local PSS is developed in the next section.

5.3 Hybrid control design

It can be seen from the previous section that the higher-frequency modes (e.g. mode A) are the ones affected most adversely by the time delays. This is expected: when the communication delay becomes comparable with the oscillatory mode period, then, controlling the mode through the WADC becomes challenging. Fortunately, in electric power systems, the higher-frequency modes are usually local modes [50] and can be efficiently tackled by local PSSs. The ones harder to tackle with local controls are the inter-area modes that might require the observation of geographically dispersed devices and the coordination of resources in various parts of the system. This separation can be exploited to design a hybrid stabilising controller.

For this hybrid control, the WADC was redesigned to focus its control effort on the slower inter-area mode B, while a local PSS was designed to improve the damping of the faster, local, mode A. For the PSS design, the well-known residues method [51] was used. Its input and output signals were selected similarly to the previous section. The SWP CCGT generator rotor speed deviation was selected as the PSS input signal, and its output was connected to the generator AVR reference. Including the local PSS controller improved the damping of mode A to 6.4% leaving the one of mode B almost unaffected (Fig. 15).
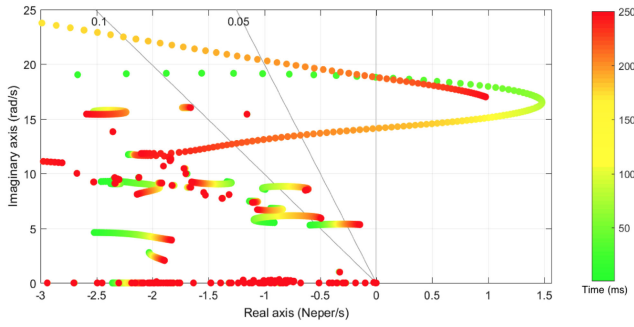
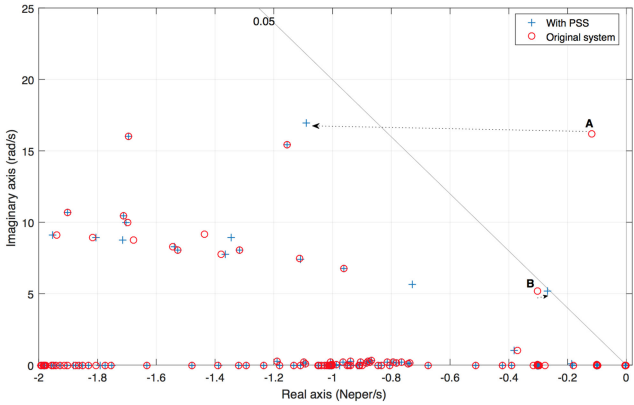**Fig. 14** *Effect of communication time delays on the controlled (only WADC) system*

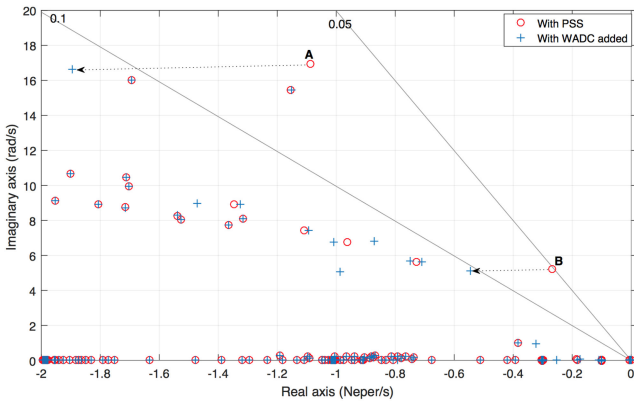**Fig. 15** *Comparison of eigenvalues between the uncontrolled and controlled (only local PSS) system*

Fig. 16 *Comparison of eigenvalues between the uncontrolled and controlled (hybrid) system*

The new WADC was designed based on the CPPS including the PSS. The WADC was synthesised focusing on the control of the inter-area mode B, modifying the previous weighting functions to

$$W_1(s) = \frac{36}{s^2 + 8.4s + 10}, \quad W_2(s) = \frac{10s}{s + 10} \quad (18)$$

The cut-off frequency of the low-pass filter was reduced to 6 rad/s to focus on frequencies below that value (that usually correspond to inter-area modes). The high-pass filter was also reduced to a lower value, resulting in a minimisation of the control effort at a lower-frequency threshold than in the previous design. The rest of the design procedure follows that of Section 5.2. Fig. 16 shows the improvement in the damping of the inter-area mode B with the hybrid control scheme. It can be seen that mode A is also significantly improved.

Similarly to the previous section, a time-delay sensitivity analysis was performed on the system with hybrid control. As can be observed in Fig. 17, the system is now more resilient to time delays. While the performance of the hybrid controller still
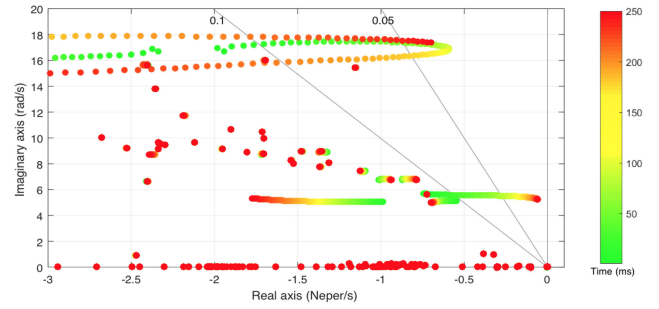

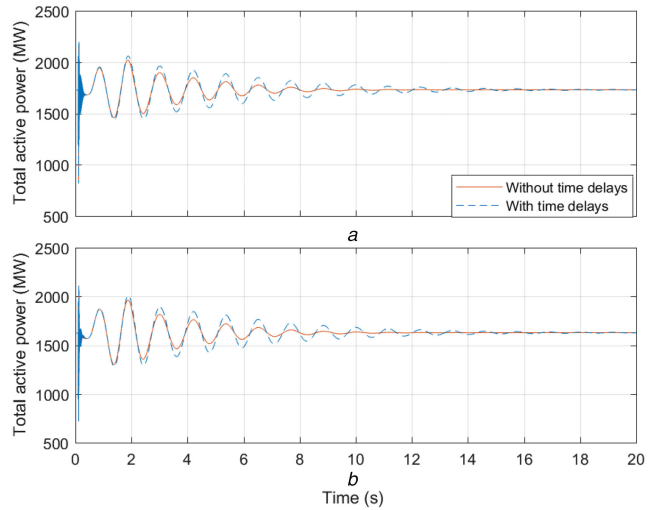**Fig. 17** *Effect of communication time delays on the controlled (hybrid) system*

Fig. 18 *Power flow from Scotland to the South for the controlled (hybrid) system, with and without communication delays*
(a) Total active power flow from Eccles (node 8) to Stella West (node 10), *(b)* Total active power flow from Strathaven (node 6) to Harker (node 9)

degrades for very large communication delays, it does not become unstable.

Fig. 18 shows the time-domain response of the active power flowing from Scotland to the South after a short-circuit is applied, when ignoring the communication delays and when considering an average background communication load. Even though there is still some degradation in performance when the time delays are considered, the CPPS is adequately damped. It should be noted that for the same conditions, the WADC designed in Section 5.2 is unstable.
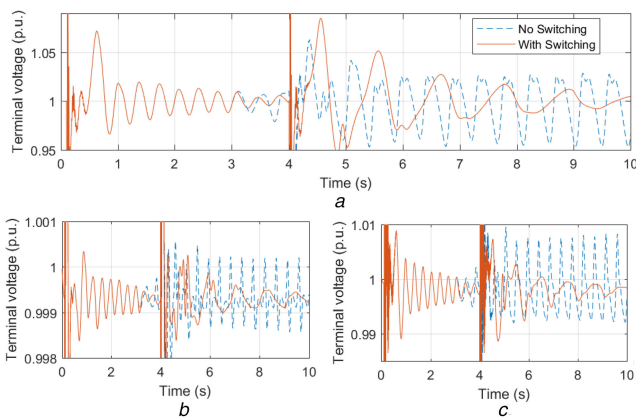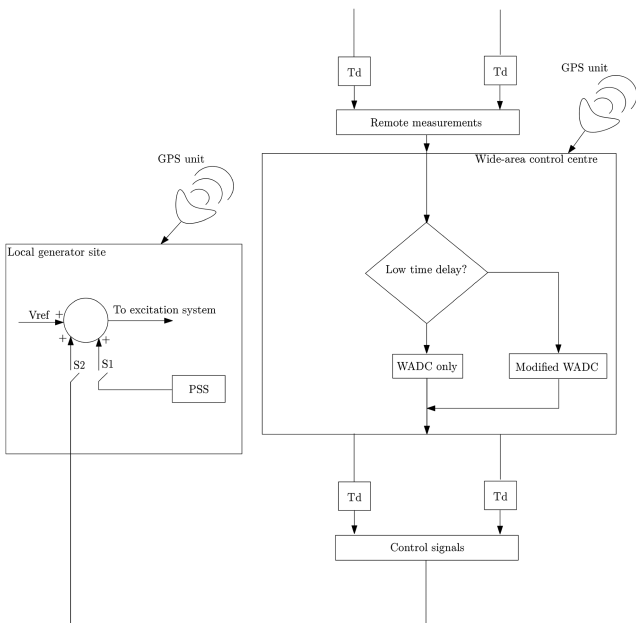
The performance of the hybrid controller is further assessed for different loading conditions in both the power and communication networks. The communication delays are computed based on the methodology explained in Section 2.2 and varying the background communication load between zero and full loading (which in this case corresponds to 137.3 ms for the link from the Beauly node to the control centre and 61.5 ms for the link from the SWP node to the control centre). At the same time, the electric power system is stressed by increasing the power transfer from Scotland to the South in equal steps of 10%.

Table 3 shows the combination of the various power and communication loading scenarios and their effect on the inter-area mode B. It can be observed that the hybrid controller provides relatively constant damping of 10.8% for all the operating conditions considered at zero latency. However, with increased power loads and the introduction of communication delays, its performance degrades, with the damping going as low as 3.42% in the most stressed scenario. For this reason, the rule-based switching strategy described in the next section is proposed.

As a hybrid model, it represents a comprise between the WADC only model and the local PSS. Hence, Its damping performance is worst than the WADC only model as evidenced by Figs. 12 and 16. Also, in situations of extreme time delays, its performance is worst than the local PSS operating alone, as illustrated in Fig. 19.

Table 3 Damping performance of the controlled (hybrid) system for mode B, under different loading conditions

Power increase, %	Communication latency	Eigenvalue	Frequency, Hz	Damping, %
10	zero delay	$-0.5582 \pm j5.137$	0.82	10.80
	max delay	$-0.2615 \pm j5.486$	0.87	4.76
20	zero delay	$-0.5682 \pm j5.158$	0.82	10.95
	max delay	$-0.2452 \pm j5.489$	0.87	4.46
30	zero delay	$-0.5745 \pm j5.179$	0.82	11.03
	max delay	$-0.2294 \pm j5.488$	0.87	4.18
40	zero delay	$-0.5784 \pm j5.202$	0.83	11.05
	max delay	$-0.2145 \pm j5.487$	0.87	3.91
50	zero delay	$-0.5779 \pm j5.227$	0.83	10.99
	max delay	$-0.2005 \pm j5.485$	0.87	3.65
60	zero delay	$-0.5696 \pm j5.252$	0.84	10.78
	max delay	$-0.1873 \pm j5.481$	0.87	3.42

Fig. 19 *Selected generator terminal voltages of the controlled system with and without control strategy switching*
(a) SWP CCGT, *(b)* Keadby coal, *(c)* Sellindge nuclear

Fig. 20 *Illustration of the proposed rule-based control strategy*

5.4 Rule-based switching control strategy

In the previous sections, it was shown that the H_∞-based WADC shows excellent performance in low communication delays but has little resilience in high communication delays that can destabilise the system. Then, a hybrid control scheme was developed that shows increased resilience to time delays by tackling the local modes with PSS and the inter-area modes with a WADC. However, the performance of the latter in low communication delays is not as good as the former. Moreover, in very high communication delays, the system performance with the hybrid method still degrades significantly.

In this section, a rule-based control strategy is shown that combines the best behaviour of the controllers, under different communication latencies. The different controllers are pre-designed offline and are switched depending on the detected time delays. This switching between controllers is done in the control system layer and can be implemented using mature adaptive control techniques such as gain scheduling [52]. The overview is shown in Fig. 20 and explained below.

For low communication latency (<60 ms), the WADC designed in Section 5.2 is used ensuring superior damping performance (switch $S1$ open and $S2$ closed). When the time delays increase beyond the point where the WADC performance is likely to be affected (>60 ms, as extracted from the sensitivity plots), the hybrid scheme is used ($S1$ and $S2$ closed but WADC concentrates only on inter-area modes). Finally, for extreme values of communication latency or even loss of communications, only local controllers (PSSs) are used to tackle both local and inter-area modes (switch $S1$ closed and $S2$ open). The last mode of operation (only local) is the current industry practise which can stabilise the system in most situations but cannot achieve the performance of WADCs.

With the aid of accurate GPS time-stamp information, the communication delays can be reliably and accurately determined locally [13, 28] and trigger the appropriate control strategy. It is thus assumed that every remote generator and the WADC centre are equipped with GPS and all signals timestamped.

Moreover, for the hybrid control strategy, several communication scenarios should be considered, where one or some communication links are overloaded (with a latency above the threshold). This can lead to multiple hybrid controllers that can be scheduled according to the actual communication scenario.

To test the impact of the switching scheme, two three-phase short-circuit faults lasting for 20 ms each are applied on node SWP at time instants $t = 0.1$ and $4\,\text{s}$ to excite the oscillatory modes. Right before the second fault, a step change in the background communication is applied to increase significantly the communication time delay between the WADC and the controlled generators.

Fig. 19 and Fig. 21 show the time-domain response of the generator speed deviations and terminal voltages with and without the switching strategy. In the first scenario, the step increase in communication latency causes the system performance to degrade. When the switching strategy is considered, then the increased communication latency is detected and the controller switches to the hybrid mode. As expected, the increased resilience of the hybrid scheme to time delays offers better damping performance with smoother oscillations.
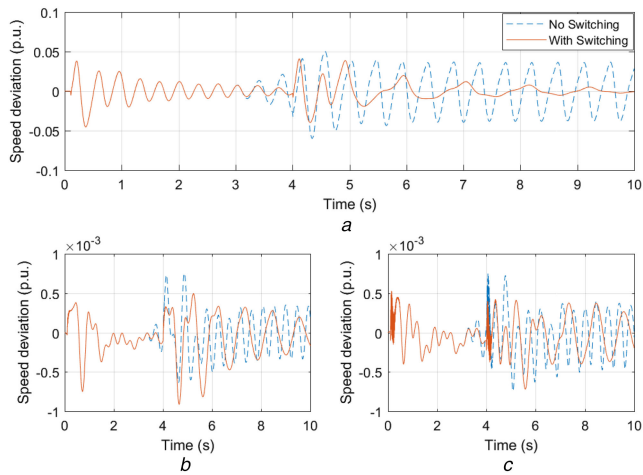
However, when analysing a wide range of communication time delays that might realistically develop in the BT 21CN, then the proposed hybrid controller shows better robustness and satisfactory performance in the entire range.

Fig. 21 *Selected generator speed deviation of the controlled system with and without control strategy switching*
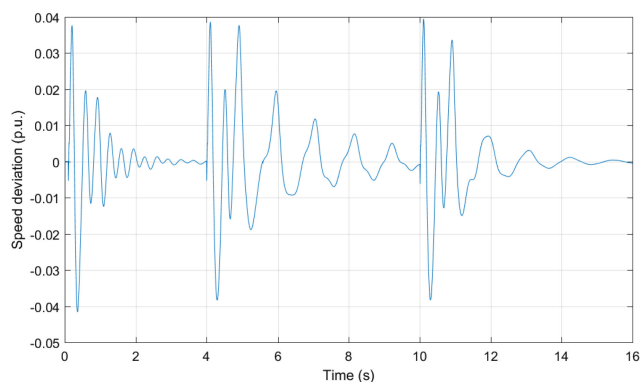*(a)* SWP CCGT, *(b)* Keadby coal, *(c)* Sellindge nuclear

Fig. 22 *SWP CCGT generator speed deviation response showing the three-stage switching*

Finally, Fig. 22 shows the speed deviation of the SWP CCGT generator when three short-circuit faults lasting for 20 ms each are applied at time instants $t = 0.1, 4,$ *and* 10 s to excite the oscillatory modes. Similarly to the previous test, right before each of the two last faults, a step change in the background communication is applied. This leads the control strategy to move from WADC to hybrid and finally local. It should be noted that the maximum time delay before the final fault increases to more than 350 ms and would destabilise the system if the WADC was used.

6 Conclusions

Electric power systems are quickly being transformed into CPPS, with the improved communication capabilities paving the way for enhanced functionalities being deployed over the cyber layer. Using public communication networks to implement the new CPPS services can significantly reduce the installation and operation cost but at the same time expose CPPS to stability problems arising from decreased performance or disturbances in the communication network.

In this paper, the design of a WADC to tackle oscillations in electric power systems is presented, based on a cyber-physical model of GB. It is shown that the enhanced monitoring and control capabilities offered in the CPPS by the communication network can significantly increase the stability of the system. However, high communication delays can destabilise the system and lead to a collapse. It was shown that the resilience of the WADC to communication latency can be increased by tackling the fast oscillatory modes with local controllers (PSS) while the WADC focuses only on the slower inter-area modes, which are usually the hardest to tackle with only local controls. Finally, a rule-based control strategy is proposed that can combine the superior performance of WADC in low-latency situations, with the

increased resilience to the latency of a hybrid method and the robustness of traditional local controls (PSS).

Immediate future work will extend the investigation of the cyber-physical system by considering a range of cyber-attack scenarios together with designing formal recovery rules for the wide-area controllers when faced with such attacks. Also, we intend to perform a more comprehensive investigation on the effect of time delays on the CPPS while considering more varied wide-area communication architectures including emerging cyber-physical architectures such as the cloud-in-the-loop architecture [53].

8 References

[1] Yu, X., Xue, Y.: 'Smart grids: a cyber-physical systems perspective', *Proc. IEEE*, 2016, **104**, (5), pp. 1058–1070
[2] Wang, W., Xu, Y., Khanna, M.: 'A survey on the communication architectures in smart grid', *Comput. Netw.*, 2011, **55**, (15), pp. 3604–3629
[3] Jain, S., Vinoth, K.N., Paventhan, A.*, et al.*: 'Survey on smart grid technologies-smart metering, IoT and EMS'. 2014 IEEE Students' Conf. Electrical, Electronics and Computer Science SCEECS 2014, Bhopal, India, 2014
[4] Nourizadeh, S., Karimi, M., Ranjbar, A.*, et al.*: 'Power system stability assessment during restoration based on a wide area measurement system', *IET Gener. Transm. Distrib.*, 2012, **6**, (11), pp. 1171–1179
[5] Vellaithurai, C.B., Biswas, S.S., Liu, R.*, et al.*: 'Real time modeling and simulation of cyber-power system', in Khaitan, S.K., McCalley, J.D., Liu, C.C. (Eds.): '*Cyber physical systems approach to smart electric power grid*' (Springer, Berlin, Heidelberg, 2015), pp. 43–74
[6] Chakrabortty, A., Khargonekar, P.P.: 'Introduction to wide-area control of power systems'. 2013 American Control Conf., Washington, D.C., USA, 2013, pp. 6758–6770
[7] Zhang, Y., Bose, A.: 'Design of wide-area damping controllers for interarea oscillations', *IEEE Trans. Power Syst.*, 2008, **23**, (3), pp. 1136–1143
[8] Li, Y., Rehtanz, C., Yang, D.*, et al.*: 'Robust high-voltage direct current stabilising control using wide-area measurement and taking transmission time delay into consideration', *IET Gener. Transm. Distrib.*, 2011, **5**, (3), p. 289
[9] Li, Y., Zhou, Y., Liu, F.*, et al.*: 'Design and implementation of delay-dependent wide-area damping control for stability enhancement of power systems', *IEEE Trans. Smart Grid*, 2017, **8**, (4), pp. 1831–1842
[10] Saputro, N., Akkaya, K., Uludag, S.: 'A survey of routing protocols for smart grid communications', *Comput. Netw.*, 2012, **56**, (11), pp. 2741–2771
[11] 'Blackout 2003: final report on the August 14, 2003 blackout in the United States and Canada: causes and recommendations'. Technical Report, Electricity Markets and Policy Group, Energy Analysis and Environmental Impacts Department, US Department of Energy, Washington, D.C., 2004. Available at https://www.energy.gov/sites/prod/files/oeprod/DocumentsandMedia/BlackoutFinal-Web.pdf, accessed on 10 August 2017
[12] Aboul-Ela, M., Sallam, A., McCalley, J.*, et al.*: 'Damping controller design for power system oscillations using global signals', *IEEE Trans. Power Syst.*, 1996, **11**, (2), pp. 767–773
[13] Chaudhuri, B., Majumder, R., Pal, B.: 'Wide-area measurement-based stabilizing control of power system considering signal transmission delay', *IEEE Trans. Power Syst.*, 2004, **19**, (4), pp. 1971–1979
[14] Li, J., Chen, Z., Cai, D.*, et al.*: 'Delay-dependent stability control for power system with multiple time-delays', *IEEE Trans. Power Syst.*, 2016, **31**, (3), pp. 2316–2326
[15] Li, T., Wu, M., He, Y.: 'Lyapunov–Krasovskii functional based power system stability analysis in environment of WAMS', *J. Cent. South Univ. Technol.*, 2010, **17**, (4), pp. 801–806
[16] Qiang, S., Haiyun, A., Hongjie, J.*, et al.*: 'An improved power system stability criterion with multiple time delays'. 2009 IEEE Power & Energy Society General Meeting, Calgary, AB, Canada, July 2009, pp. 1–7
[17] Milano, F., Anghel, M.: 'Impact of time delays on power system stability', *IEEE Trans. Circuits Syst. I, Regul. Pap.*, 2012, **59**, (4), pp. 889–900
[18] Jarlebring, E., Damm, T.: 'The Lambert W function and the spectrum of some multidimensional time-delay systems', *Automatica*, 2007, **43**, (12), pp. 2124–2128
[19] Zhang, S., Vittal, V.: 'Design of wide-area power system damping controllers resilient to communication failures', *IEEE Trans. Power Syst.*, 2013, **28**, (4), pp. 4292–4300
[20] Olgac, N., Sipahi, R.: 'An exact method for the stability analysis of time-delayed linear time-invariant (LTI) systems', *IEEE Trans. Autom. Control*, 2002, **47**, (5), pp. 793–797
[21] Ye, H., Liu, Y., Zhang, P.: 'Efficient eigenanalysis for large delayed cyber-physical power system using explicit infinitesimal generator discretization', *IEEE Trans. Power Syst.*, 2016, **31**, (3), pp. 2361–2370

[22] Gao, W., Ye, H., Liu, Y., *et al.*: 'Comparison of three stability analysis methods for delayed cyber-physical power system'. 2016 China Int. Conf. Electricity Distribution (CICED), Xi'an, Shaanxi Province, China, August 2016, vol. 2016-Septe, no. Ciced, pp. 1–5

[23] Zabaiou, T., Dessaint, L.-A., Okou, F.-A., *et al.*: 'Wide-area coordinating control of SVCs and synchronous generators with signal transmission delay compensation'. IEEE PES General Meeting, Providence, RI, USA, July 2010, pp. 1–9

[24] Wu, H., Tsakalis, K., Heydt, G.: 'Evaluation of time delay effects to wide-area power system stabilizer design', *IEEE Trans. Power Syst.*, 2004, **19**, (4), pp. 1935–1941

[25] Ke, D.P., Chung, C.Y., Xue, Y.: 'An eigenstructure-based performance index and its application to control design for damping inter-area oscillations in power systems', *IEEE Trans. Power Syst.*, 2011, **26**, (4), pp. 2371–2380

[26] Shah, R., Mithulananthan, N., Lee, K.Y.: 'Large-scale PV plant with a robust controller considering power oscillation damping', *IEEE Trans. Energy Convers.*, 2013, **28**, (1), pp. 106–116

[27] Preece, R., Milanovic, J.V., Almutairi, A.M., *et al.*: 'Probabilistic evaluation of damping controller in networks with multiple VSC-HVDC lines', *IEEE Trans. Power Syst.*, 2013, **28**, (1), pp. 367–376

[28] Zhang, P., Yang, D., Chan, K., *et al.*: 'Adaptive wide-area damping control scheme with stochastic subspace identification and signal time delay compensation', *IET Gener. Transm. Distrib.*, 2012, **6**, (9), p. 844

[29] Wang, J.K., Peng, C.: 'Analysis of time delay attacks against power grid stability'. Proc. Second Workshop on Cyber-Physical Security and Resilience in Smart Grids – CPSR-SG'17, New York, New York, USA, 2017, pp. 67–72

[30] Goebel, R., Sanfelice, R., Teel, A.: 'Hybrid dynamical systems', *IEEE Control Syst.*, 2009, **29**, (2), pp. 28–93

[31] Mueller, S.C., Georg, H., Nutaro, J., *et al.*: 'Interfacing power system and ICT simulators: challenges, state-of-the-art, and case studies', *IEEE Trans. Smart Grid*, 2016, **PP**, (99), p. 1

[32] Belivanis, M., Bell, K.: 'Representative GB network model: notes'. Technical Report, University of Strathclyde, Glasgow, Scotland, 2011

[33] Anderson, P.M., Fouad, A.A.: '*Power system control and stability*' (Wiley-IEEE Press, USA, 2002, 2nd edn.)

[34] 'Dynamic models for steam and hydro turbines in power system studies'. Technical Report 6, November 1973

[35] Kitz: 'BT 21CN – network topology', 2018. Available at https://kitz.co.uk/adsl/21cn_network.htm

[36] BT: '21CN network topology', 2007. Available at http://www.btwholesale.com/content/binaries/21_Century_Network_Community/NSWG -Material 3 July 07 v5.zip, accessed on 10 August 2017

[37] Samitier, C.: '*Utility communication networks and services: specification, deployment and operation*' (Springer, Switzerland, 2016)

[38] Shen, G., Tucker, R.S.: 'Energy-minimized design for IP over WDM networks', *J. Opt. Commun. Netw.*, 2009, **1**, (1), p. 176

[39] Csoma, A., Toka, L., Gulyas, A.: 'On lower estimating Internet queuing delay'. 2015 38th Int. Conf. Telecommunications and Signal Processing TSP 2015, Prague, Czech Republic, 2015, pp. 299–303

[40] Elmirghani, J.M.H., Klein, T., Hinton, K., *et al.*: 'Greentouch GreenMeter core network energy-efficiency improvement measures and optimization', *J. Opt. Commun. Netw.*, 2018, **10**, (2), p. A250

[41] Vinod, J., Brett, C.: '*Deploying QoS for cisco IP and next generation networks: the definitive guide*' (Elsevier, USA, 2009). Available at http://linkinghub.elsevier.com/retrieve/pii/B9780123744616X00018

[42] Infinera: 'Low latency – how low can you go ?' White Paper, 2015

[43] Cisco Systems: 'Cisco ONS 15501 erbium doped fiber amplifier data sheet'. Technical Report Available at http://cicsno.com

[44] Glimmerglass: 'Intelligent optical system 600', 2013. Available at http://www.glimmerglass.com/products/intelligent-optical-systems, accessed on 12 October 2017

[45] Younis, M.R., Iravani, R.: 'Wide-area damping control for inter-area oscillations: a comprehensive review'. 2013 IEEE Electrical Power & Energy Conf., Halifax, NS, Canada, August 2013, pp. 1–6

[46] Pal, B., Chaudhuri, B.: '*Robust control in power systems*', ser. power electronics and power systems (Springer, Boston, USA, 2005)

[47] Lin, F.: '*Robust control design*', ser. RSP series in control theory and applications (John Wiley & Sons, Ltd., Chichester, UK, 2007)

[48] Glover, K., Doyle, J.C.: 'State-space formulae for all stabilizing controllers that satisfy an H-inf-norm bound and relations to relations to risk sensitivity', *Syst. Control Lett.*, 1988, **11**, (3), pp. 167–172

[49] Mendoza-Armenta, S., Dobson, I.: 'Applying a formula for generator redispatch to damp interarea oscillations using synchrophasors', *IEEE Trans. Power Syst.*, 2016, **31**, (4), pp. 3119–3128

[50] Kundur, P., Kundur, P.: '*Power system stability and control*' (McGraw-Hill Education, USA, 1994)

[51] Gibbard, M., Pourbeik, P., Vowles, D.: '*Small-signal stability, control and dynamic performance of power systems*' (University of Adelaide Press, Adelaide, 2015)

[52] Åström, K.J., Wittenmark, B.: '*Adaptive control*' (Courier Corporation, USA, 2013)

[53] Soudbakhsh, D., Chakrabortty, A., Annaswamy, A.M.: 'A delay-aware cyber-physical architecture for wide-area control of power systems', *Control Eng. Pract.*, 2017, **60**, pp. 171–182